RESEARCH ARTICLE

WILEY

A high-density 256-channel cap for dry electroencephalography

Patrique Fiedler[1] [iD] | Carlos Fonseca[2,3] [iD] | Eko Supriyanto[4] [iD] | Frank Zanow[5] |
Jens Haueisen[1,6] [iD]

[1]Institute of Biomedical Engineering and Informatics, Technische Universität Ilmenau, Ilmenau, Germany

[2]Faculdade de Engenharia, Departamento de Engenharia Metalúrgica e de Materiais, Universidade do Porto, Porto, Portugal

[3]LAETA/INEGI, Institute of Science and Innovation in Mechanical and Industrial Engineering, Porto, Portugal

[4]IJN-UTM Cardiovascular Engineering Centre, Universiti Teknologi Malaysia, Johor Bahru, Malaysia

[5]eemagine Medical Imaging Solutions GmbH, Berlin, Germany

[6]Department of Neurology, Biomagnetic Center, University Hospital Jena, Jena, Germany

Correspondence
Patrique Fiedler, Institute of Biomedical Engineering and Informatics, Technische Universität Ilmenau, 98693 Ilmenau, Germany.
Email: patrique.fiedler@tu-ilmenau.de

Abstract

High-density electroencephalography (HD-EEG) is currently limited to laboratory environments since state-of-the-art electrode caps require skilled staff and extensive preparation. We propose and evaluate a 256-channel cap with dry multipin electrodes for HD-EEG. We describe the designs of the dry electrodes made from polyurethane and coated with Ag/AgCl. We compare in a study with 30 volunteers the novel dry HD-EEG cap to a conventional gel-based cap for electrode-skin impedances, resting state EEG, and visual evoked potentials (VEP). We perform wearing tests with eight electrodes mimicking cap applications on real human and artificial skin. Average impedances below 900 kΩ for 252 out of 256 dry electrodes enables recording with state-of-the-art EEG amplifiers. For the dry EEG cap, we obtained a channel reliability of 84% and a reduction of the preparation time of 69%. After exclusion of an average of 16% (dry) and 3% (gel-based) bad channels, resting state EEG, alpha activity, and pattern reversal VEP can be recorded with less than 5% significant differences in all compared signal characteristics metrics. Volunteers reported wearing comfort of 3.6 ± 1.5 and 4.0 ± 1.8 for the dry and 2.5 ± 1.0 and 3.0 ± 1.1 for the gel-based cap prior and after the EEG recordings, respectively (scale 1–10). Wearing tests indicated that up to 3,200 applications are possible for the dry electrodes. The 256-channel HD-EEG dry electrode cap overcomes the principal limitations of HD-EEG regarding preparation complexity and allows rapid application by not medically trained persons, enabling new use cases for HD-EEG.

KEYWORDS
biopotential electrode, dry electrode, EEG, EMG, mobile EEG, wearable biomedical sensors

1 | INTRODUCTION

Electroencephalography (EEG) is widely used in both clinical neurology and neuroscientific research. Recent developments of highly compact, lightweight, and battery-powered commercial biosignal amplifier electronics have fostered progress in a multitude of new fields of application for EEG. Nowadays, EEG is increasingly used for studying individual brain function, brain–body interaction, and emotional, psychological, and social group interaction outside conventional lab setups in highly mobile, ecological environments (Astolfi et al., 2010; Filho, Bertollo, Robazza, & Comani, 2015; Lau-Zhu, Lau, & McLoughlin, 2019; Makeig, Gramann, Jung, Sejnowski, & Poizner, 2009).

Gel-based silver/silver-chloride (Ag/AgCl) electrodes represent an often-used standard for electrophysiological measurements (Searle & Kirkup, 2000). The electrode-skin contact for gel-based electrodes is mediated by an electrolyte gel or paste which is manually applied at each electrode position. Skin preparation, gel application, and subsequent cleaning require skilled personnel and extensive laboratory time. The complexity and time requirements cause the overall preparation process to be error-prone, eventually leading to falsified measurements due to damaged or misplaced electrodes or gel-bridges between adjacent channels. The impact of these disadvantages and the prevalence of errors considerably increase with electrode number and density, especially in high-density EEG (HD-EEG) setups with 256 electrodes. Moreover, the preparation procedure and gel drying effects hamper the application in mobile and group applications (di Flumeri et al., 2019; Kleffner-Canucci, Lu, Naveway, & Tucker, 2012).

Dry electrodes rely on direct electrode-skin contact, eliminating gel application requirements. Moreover, dry electrodes—in contrast to gel-based electrodes—can be self-applied by the user. Different concepts of dry electrodes have been proposed for EEG, including flat adhesive patches (Lepola et al., 2014, Bleichner & Debener, 2017, Fu et al. 2020, Zhang et al., 2020), pin-shaped (Chen et al., 2014; di Flumeri et al., 2019; Fiedler et al., 2015; Hinrichs et al., 2020; Kimura, Nakatani, Nishida, Taketoshi, & Araki, 2020), spider-shaped (Mullen et al., 2015), and brush electrodes (Grozea, Voinescu, & Fazli, 2011; Kimura et al., 2020). Similarly, the material compositions vary significantly from solid metals (Fiedler et al., 2014; Hinrichs et al., 2020) to intrinsically conductive polymer composites (Bradford et al., 2018; Chen et al., 2014; Zhang et al., 2020), and coated polymers (Fiedler et al., 2015; Fu et al., 2020; Kimura et al., 2020; Mota et al., 2013). To date, the majority of dry electrodes are applied in low-density EEG with up to 32 channels only, due to physical or cost limitations (e.g., electrode size; required electrode adduction mechanisms; electronics for active electrodes [Fonseca et al., 2007; Marini, Lee, Wagner, Makeig, & Gola, 2019; Patki et al., 2012; Xu, Mitra, van Hoof, Yazicioglu, & Makinwa, 2017]).

HD-EEG uses considerably more electrodes than conventional clinical EEG, in order to provide a high spatial sampling of the potential distribution on the head. The information gain has been discussed extensively in the literature and has been shown to support source localization accuracy (Sohrabpour et al., 2016; Stoyell et al., 2021) and connectivity analysis (Liu, Ganzetti, Wenderoth, & Mantini, 2018); contribute to the analysis of temporal EEG dynamics (Robinson et al., 2017), and phase synchronization (Ramon & Holmes, 2015; Ramon & Holmes, 2020). Beyond research, the increasing use and benefit of HD-EEG have also been highlighted in clinical applications, improving identification of epileptic fast oscillations and localization of seizure onset zones (Sohrabpour et al., 2016, Stoyell et al., 2021); supporting monitoring of disease-progression biomarkers like evoked potentials (Lascano, Lalive, Hardmeier, Fuhr, & Seeck, 2017); supporting concurrent MEG/EEG (Puce & Hämäläinen, 2017). Moreover, specifically dry electrode setups profit from increased spatial resolution, allowing for spatial over-sampling to be used for artifact

detection and correction (Graichen et al., 2015; Larson & Taulu, 2017; Tamburro, Fiedler, Stone, Haueisen, & Comani, 2018) and compensating the currently lower channel reliability of dry electrodes.

We present a novel 256-channel cap with semi-flexible, multipin-shaped, dry electrodes, with specifically adapted size, pin number, and electrode layout for HD-EEG. Three different electrode types are integrated for easy, reproducible, and comfortable electrode-skin contact at hairy (long pins), less hairy (medium pins), and non-hairy (wave pins) positions. We compare the performance and applicability of the novel dry HD-EEG cap to a standard gel-based HD-EEG cap in a study on 30 healthy volunteers. We apply an established benchmarking paradigm allowing direct comparison of the results with previous low-density dry EEG studies. Additionally, we present wearing tests investigating the durability of the dry electrodes.

2 | MATERIALS AND METHODS

2.1 | Electrodes and caps

The novel electrodes were developed based on our previous dry electrodes (Fiedler et al., 2015; Fiedler et al., 2018) and adopted for smaller overall diameter and consequently reduced pin number, allowing for a higher channel count compared to our previous EEG caps. These novel multipin electrodes comprise an overall number of 19 pins integrated on one common baseplate. As shown in Fiedler et al., 2018, 19 pin electrodes can establish a reliable and reproducible electrode-skin contact. Although Fiedler et al., 2018 used electrodes with larger baseplate diameter in a dual-electrode measurement setup, the pin shape, pin arrangement, and pin distance were identical to the HD-EEG electrodes used in the current study. Consequently, the relevant functional components of the electrodes are identical and can be directly compared. Three electrode types are derived: Two pin-shaped electrodes with a pin length of 6 and 3 mm, respectively applied to head regions with dense and less dense hair (anterior positions). The third electrode type (wave pins) comprises a flat surface with 19 half-spheres of 1.5 mm diameter on top, specifically addressing the non-hairy positions at the forehead (see Figure 1c,e). These three basic designs aim to provide a good compromise between the electrode's capabilities to easily pass through the hair, establish a reliable and reproducible electrode-skin contact, and provide sufficient wearing comfort for the user (di Fronso et al., 2019).

Thermoset Polyurethane (Biresin U1419, Sika Chemie GmbH, Bad Urach, Germany) with a Shore A hardness of 98 serves as the semi-rigid electrode substrate material and allows adaptation to the local head curvature, avoiding excessive, painful local pressure spots (Cuadrado et al., 2009; Fiedler et al., 2018). An Ag/AgCl coating provides electrical conductivity and reliable electrochemical characteristics. The coating is applied to the nonconductive PU substrate utilizing a multi-phase electroless plating technique (Fiedler et al., 2015; Mota et al., 2013) ensuring a highly conductive coating as well as adhesion between coating and substrate. This approach enables the reusability of the electrodes. Both the substrate and the

FIGURE 1 Compared electrode and cap types: (a) dry electrode cap, and (b) commercial gel-based cap shown outside (left) and turned inside-out (right); (c) dry electrode types with wave, medium, long pins, and (d) gel-based sintered Ag/AgCl electrode; (e) equidistant electrode layout with 256 channels + reference and patient ground; including color-coded positions of the different electrode types
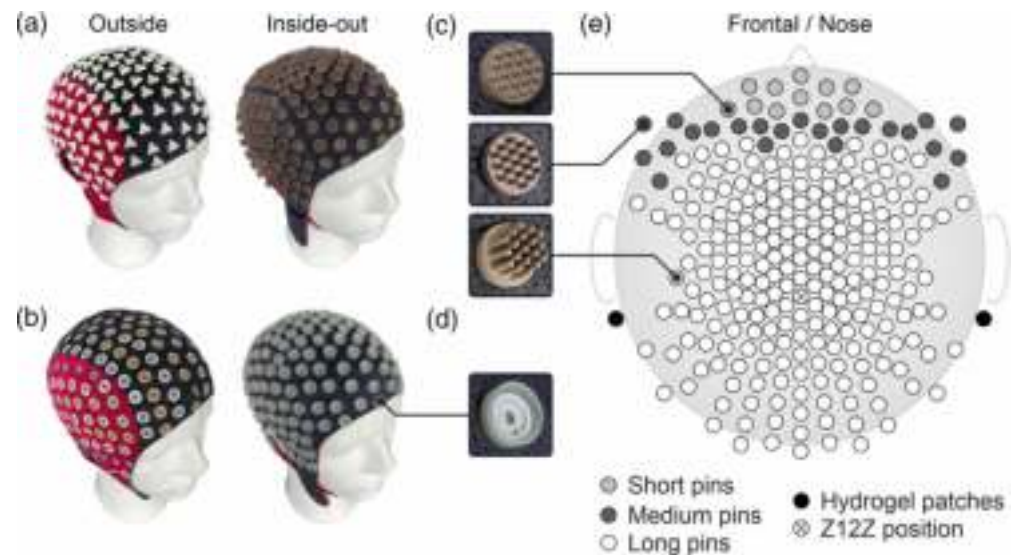
coating material have passed biocompatibility tests for use on healthy skin.

Coaxial cables are soldered directly to the back of the electrodes, supporting the use of active shielding for reduced susceptibility to environmental noise (van Rijn, Peper, & Grimbergen, 1990). The 256 dry electrodes are integrated into a double-layer fabric cap. Cabling is covered completely between the two fabric layers avoiding exposure to mechanical stress during application and removal of the cap. All electrodes are mechanically fixated in the cap at equidistant positions as shown in Figure 1e. The equidistant layout was chosen because of its advantages in the mechanical characteristics and thus adaptivity of the cap to different head shapes as well as for data analysis including spatial filtering (Graichen et al., 2015), calculation of connectivity measures, or source reconstruction as commonly done in HD-EEG data analysis. Reference and patient ground electrodes are integrated as flat-snap dropleads at the right and left mastoid, respectively, intended for using self-adhesive replaceable patch electrodes. An image of the overall cap is shown in Figure 1a both from the outside (left) and turned inside-out (right image).

For the acquisition of reference data, we used a commercial gel-based cap (waveguard™ original CA-205, ANT Neuro BV, Hengelo, Netherlands) comprising sintered Ag/AgCl electrodes with coaxial cabling arranged in the same equidistant electrode layout. Here, the reference electrode was placed near the vertex at Z12Z position (see Figure 1e), resulting in overall 255 referential EEG channels. The integrated Ag/AgCl patient ground droplead electrode was placed at the left mastoid using adhesive medical tape.

2.2 | In-vivo measurements

The novel dry electrode and the commercial gel-based HD-EEG caps were compared using our previously established validation paradigm (Fiedler et al., 2015) for assessment and comparison of:

1. Preparation time measured between the initial cap application on the volunteer's head and the start of the EEG recordings;
2. Signal quality of (a) eyes-open and (b) eyes-closed resting state EEG, (c) eye blinks, and (d) pattern reversal visual evoked potentials (VEP);
3. Electrode-skin impedances and channel offset potentials at the beginning and end of the EEG acquisitions, measured with the integrated functions of the EEG amplifier;
4. Subjective wearing comfort evaluation and attention level of the volunteers prior and after the EEG acquisitions using the Scott and Huskisson pain scale, ranging from 1 to 10 (Scott & Huskisson, 1976), and the Standford sleepiness scale, ranging from 1 to 8 (Hoddes, Dement, & Zarcone, 1972), respectively.

To minimize operator-induced bias on the results, four operators performed the measurements independently. Each operator received supervised training on two volunteers. These training sessions and volunteers were excluded from data analysis.

Thirty volunteers participated in the study. VEP measurements were conducted for 20 out of the 30 volunteers. All volunteers were male, with an average age of 31 ± 10 years, an average head circumference of 58 ± 1 cm, and an average estimated hair length of 4 ± 3 cm. All volunteers consequently fall into one consistent cap size. The volunteers reported a healthy neurological, psychological, and dermatological state, no history of drug abuse, and a minimum of 7 hr of sleep the night prior to their study participation. The volunteers were asked to wash their hair using pH-neutral shampoo on the morning of the day of their study participation. Dry and gel-based recordings were performed with a minimum pause of 1 hr in-between. In each case, the dry electrode cap was applied and all related data acquisitions were performed prior to the gel-based cap. This specific test sequence and the recovery period in-between the tests were intended to minimize cross-condition influences due to skin irritation or hydration effects of the electrodes and/or electrolytes. The study complied with the ethical standards outlined in the Declaration of

Helsinki and was approved by the local Ethics Committee. All volunteers provided written informed consent before they participated in the study.

Before the application of the caps, the left (both caps) and right (dry electrode cap only) mastoids were cleaned using ethanol-soaked cotton pads. No further dedicated skin cleaning was performed at other electrode positions. For measurements with the gel-based cap, the patient ground droplead electrode was attached to the left mastoid and filled with electrolyte gel (Electro-Gel, Electro-Cap International Inc., Eaton). Subsequently, the reference electrode and the remaining EEG electrodes were gelled. During the preparation of the gel-based cap, impedance values were continuously monitored and a maximum threshold of 50 kΩ for 90% of the channels was defined. The remaining 10% of the channels should exhibit an impedance level as low as possible, while generally avoiding gel-bridges between adjacent electrodes due to eventual excessive gel application or spreading. For the dry electrode cap measurements, self-adhesive pre-gelled hydrogel electrodes (Kendall ECG electrodes H124SG, Covidien LLC, Mansfield) were applied to the patient ground and reference flat-snap dropleads and attached to the left and right mastoids, respectively. An impedance threshold of 50 kΩ was defined for the hydrogel patient ground and reference electrodes only. No impedance threshold was defined for other electrodes of the dry electrode cap. The operators were instructed to optimize the fit and electrode contact of the dry electrode cap both on a global and an individual level, by subjective evaluation of signal quality and contact reliability.

The caps were connected to four commercial mobile 64-channel referential DC-EEG amplifiers (eego™ amplifier EE-225, ANT Neuro BV, Hengelo, Netherlands) in a cascaded HD-EEG setup. This amplifier provides an input impedance >1 GΩ, a Common Mode Rejection Ratio of >100 dB, and supports active shielding. A sampling rate of 1,024 samples/s was used throughout the EEG recordings. Indications for eye blinks as well as pattern reversal stimulation for the VEP have been presented using a separate computer running eevoke software (eemagine Medical Imaging Solutions GmbH, Berlin, Germany).

2.3 | Data analysis

EEG and impedance data were recorded using the eego™ control software (ANT Neuro BV, Hengelo, Netherlands). All data were exported raw and further analyzed using custom MATLAB scripts (The Mathworks, Natick). All EEG recordings per volunteer and cap have been analyzed individually.

Impedances were analyzed for two time points: prior to the first and after the last EEG recording. Based on the manufacturer's default threshold, an upper threshold of 1 MΩ was applied to the results, also limiting the impact of measurement outliers.

We used DC-EEG amplifiers. Therefore, channel offsets were calculated as the mean over a raw data sequence of 30 s length, skipping the first 10 s of the recording to allow the electrodes to stabilize.

The recordings have been bandpass filtered using forward-backward filtering applying a 30th order Butterworth filter with cut-off frequencies at 1 and 40 Hz. Subsequently, bad channels were visually identified by independent, trained operators and excluded from further analysis of signal characteristics. Bad channels were defined as either (a) saturated, isoelectric channels, or (b) comprising artifactual, non-physiological data for more than 20% of the analyzed EEG sequence. The remaining channels were re-referenced to common average reference.

The total number of recordings in our study was 120 (30 volunteers × 4 recordings). For all EEG recordings, each channel was individually graded as either a good or bad channel according to the aforementioned definition. The relative channel reliability CR of a specific channel is defined according to Equation (1) with g being the number of EEG recordings this specific channel was marked as a good channel out of $m = 120$ overall EEG recordings per electrode type.

$$CR = \frac{g}{m} \qquad (1)$$

Furthermore, we calculated Spearman's rank correlation coefficient between groups of channels exhibiting an impedance $Z > Z_T$ (with Z_T ranging from 10 kΩ to 1 MΩ in steps of 10 kΩ) and channel groups exhibiting a channel reliability $CR < CR_T$ (with CR_T ranging from 100 to 40% in steps of 1%).

Analysis in frequency domain was performed for sequences of 30 s length of the resting state EEG recordings. Power spectral density was calculated using the Welch estimation method. The mean power of the alpha band (8–13 Hz) was calculated for each channel. Missing data for bad channels were interpolated using spherical spline interpolation (Perrin, Pernier, Bertrand, & Echallier, 1989).

The VEP results have been evaluated by averaging 150 stimulation trials per volunteer, using a pre-stimulus interval of 100 ms and a post-stimulus interval of 400 ms. The offset was determined and subtracted individually per channel as the mean value for an interval of 50 ms starting 100 ms pre-stimulus. To quantitatively compare the VEP traces of the gel-based and the dry caps, we calculated the Root Mean Square Deviation (RMSD) and the Spearman's rank correlation coefficient ρ according to Equations (2) and (3), respectively, for each channel. Herein, U corresponds to the data sample i of channel j for the gel-based (Ug) or dry (Ud) electrode recordings, respectively, out of overall $n = 513$ data samples (i.e., 500 ms of data).

$$RMSD_j = \sqrt{\frac{\sum_{i=1}^{n} \left(Ug_{ij} - Ud_{ij} \right)^2}{n}} \qquad (2)$$

$$\rho_j = \frac{\sum_{i=1}^{n} \left(Ug_{ij} - \overline{Ug} \right) \left(Ud_{ij} - \overline{Ud} \right)}{\sqrt{\sum_{i=1}^{n} \left(Ug_{ij} - \overline{Ug} \right)^2 \sum_{i=1}^{n} \left(Ud_{ij} - \overline{Ud} \right)^2}} \qquad (3)$$

The Global Field Power in the time domain (GFPt) across all channels was calculated for the VEP according to Equation (4) (Skrandies & Lehmann, 1982), with U being a voltage sample of channel m or n out of overall x channels.

$$GFPt = \sqrt{\frac{1}{2x}\sum_{m=1}^{x}\sum_{n=1}^{x}(U_m - U_n)^2} \qquad (4)$$

The $RMSD_{GFPt}$ and ρ_{GFPt} were calculated between the GFPt of both cap types for each volunteer according to Equations (5) and (6), respectively.

$$RMSD_{GFPt} = \sqrt{\frac{\sum_{i=1}^{513}(GFPtg_i - GFPtd_i)^2}{n}} \qquad (5)$$

$$\rho_{GFPt} = \frac{\sum_{i=1}^{513}(GFPtg_i - \overline{GFPtg})(GFPtd_i - \overline{GFPtd})}{\sqrt{\sum_{i=1}^{513}(GFPtg_i - \overline{GFPtg})^2 \sum_{i=1}^{513}(GFPtd_i - \overline{GFPtd})^2}} \qquad (6)$$

Two signal-to-noise ratio (SNR) estimations were derived: SNR_{GFPt} is the ratio of the GFPt at the N75 or P100 peaks and the noise power defined as the mean of the GFPt in the baseline interval $t = [-100, -50]$ ms. SNR_{max} is the ratio of the peak amplitude of the N75 or P100 to the standard deviation of the baseline interval calculated for the respective channel with maximum absolute amplitude.

The subjective attention levels, comfort evaluations, VEP peak latencies, VEP peak powers, and SNRs as well as the PSDs of all respective volunteers, have been tested for statistically significant differences between the gel-based and the dry recordings. Moreover, the spatial distribution of the alpha band power and the VEP peak amplitudes have been tested both on the level of individual channels and on the level of interpolated 2D topographies. For all aforementioned parameters, the hypothesis of a normal distribution was rejected by corresponding Kolmogorov–Smirnov tests at an alpha level of .05. Therefore, the statistical significance of the parameter differences was tested using Wilcoxon-Mann–Whitney U tests with an alpha level of .05. In the case of the PSDs compared for the frequency band 1–40 Hz in steps of 1 Hz, we applied a Bonferroni correction for post-hoc pairwise comparisons, resulting in a corrected alpha level of .0013.

2.4 | Wearing tests

The electroless plating of the PU substrates results in an Ag/AgCl layer thickness varying between 6 and 14 μm (Fiedler, 2017). Repeated applications of the cap will remove small amounts of the coating due to the friction when placing the cap on the head. Thus, the question arises of how many applications are possible until the coated layer is worn off, exposing the nonconductive substrate. We tested the durability of the coating by measuring the electrical resistance (87 III True RMS Multimeter, Fluke AG, Everett) between each of the 19 pin tips and the back of the baseplate for each of the 11 test electrodes. The test electrodes were spare samples from the production of the cap (1 wave pin and 10 long pin electrodes). These samples were produced together with and therefore identical to the electrodes in the cap.

Two different wearing tests were performed:

1. Rubbing the test electrode over a distance of 15 cm on a hairy male forearm. While this test is mimicking one manual application of the electrodes, it has inherent variability in the applied pressure and movement pattern.
2. Artificial skin was placed on a rotating plate and the test electrode was placed with a constant force of 2.9 N (300 g) on top. The electrode was positioned such that one rotation yielded also 15 cm in length for the center pin. The speed was set to 5 rpm. The artificial skin was prepared according to Dąbrowska et al. (2017) and replaced for each electrode test sample.

Standard gel-based EEG caps with sintered Ag/AgCl electrodes have an indicated lifetime of about 800 applications. Consequently, we tested our electrodes for a minimum of 800 applications (i.e., 800 rubbings on the forearm and 800 rotations on artificial skin, respectively). Given the result that after 800 applications the electrical resistance of our first test samples did not change, we extended the wearing tests to 1,600, 2,800, and 3,200 applications. For the assessment of the wearing effects, additional SEM surface images were performed (Auriga 60, Carl Zeiss Microscopy GmbH, Jena, Germany). One of the 11 electrodes was imaged directly after production and not used for the wearing tests (Condition 0 in Table 1). A summary of the tested conditions including electrode pin type, skin type, number of applications tested, and analysis performed is provided in Table 1.

## 3 | RESULTS

3.1 | Impedances and channel reliability

The grand averages of the electrode-skin impedances prior to the first EEG recording are shown in Figures 2 and 3 for the dry and gel-based recordings, respectively. The mean electrode-skin impedance across all dry electrode channels is 532 ± 199 kΩ at the beginning and 568 ± 202 kΩ at the end of the experiment. The topographies both of the mean and the standard deviation exhibit lower values at the frontal, anterior, and temporal areas, with the highest impedances in the central, parietal, and neck region of the head. On the contrary, no head regions with generally increased or decreased impedance levels are visible for the gel-based electrodes. The mean at the beginning and end of the gel-based EEG recordings is 24 ± 18 kΩ and 19 ± 14 kΩ, respectively.

The mean and standard deviation of the gel-based recordings' offset potential at the beginning and the end of the EEG recordings is −1.7 ± 30.5 mV and −0.6 ± 31.2 mV, respectively. The mean offset of the dry electrodes is 7.1 ± 46.6 mV at the beginning and 8.4 ± 53.3 mV at the end of the EEG recordings.

Based on the results of the bad-channel evaluations, the relative channel reliability was calculated across all 30 volunteers and all EEG recordings. The topographic distribution of the resulting reliability per channel is shown in Figure 4. The mean channel reliability is 84 ± 11%

Condition no.	Pin type	Skin type	No. of applications	No. of samples	Analysis method
0	Long	Not applicable	0	1	Impedance & SEM
1	Long	Real	800	2	Impedance & SEM
2	Long	Real	1,600	1	Impedance & SEM
3	Long	Real	2,800	1	Impedance
4	Long	Real	3,200	4	Impedance
5	Wave	Real	3,200	1	Impedance & SEM
6	Long	Artificial	3,200	1	Impedance & SEM
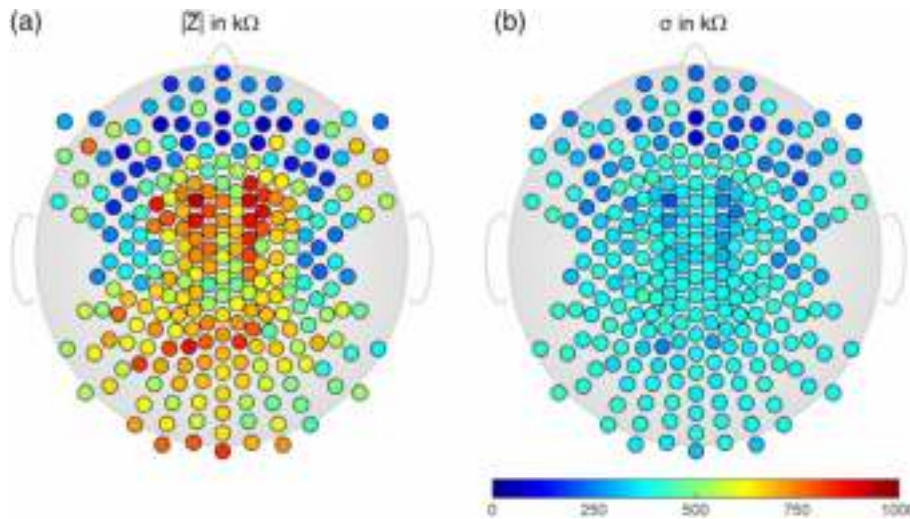
FIGURE 2 Topographic distribution of the electrode-skin impedances of the dry electrode cap at the beginning of the EEG recordings: (a) mean, and (b) SD across all volunteers
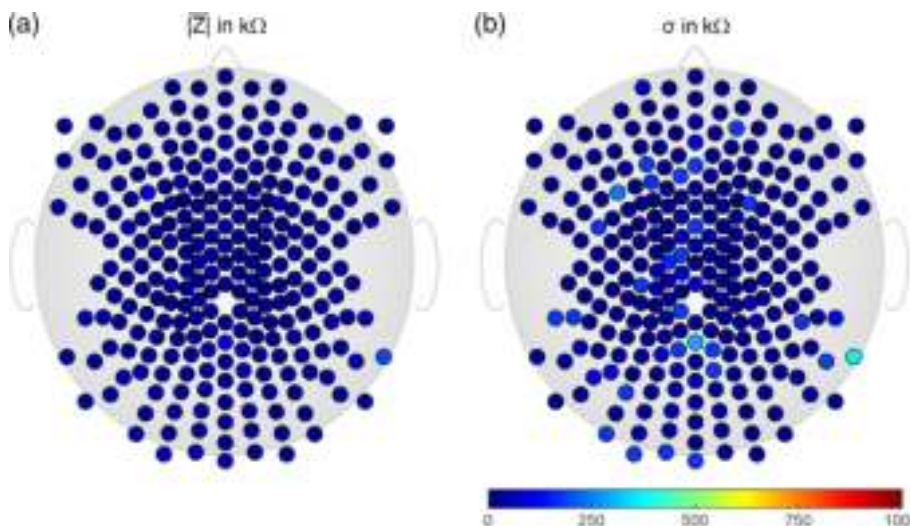

FIGURE 3 Topographic distribution of the electrode-skin impedances of the gel-based electrode cap at the beginning of the EEG recordings: (a) mean, and (b) SD across all volunteers

and 97 ± 3% for the dry and gel-based electrode cap, respectively. In line with the regions of increased electrode-skin impedance, the dry electrode cap shows reduced electrode reliability, especially at the central, parietal, and neck regions. Regions of decreased channel reliability are also visible for the gel-based cap, specifically at the frontal and parietal head regions.

Figure 5 displays the results for the correlation between groups of channels above electrode skin impedance Z_T (10 kΩ–1 MΩ, steps of 10 kΩ) and below channel reliability threshold CR_T (100–40%, steps of 1%). For impedance threshold $Z_T = 900$ kΩ, and channel reliability threshold $CR_T = 55\%$ the correlation is 1. Moreover, if the impedance is below 900 kΩ, the corresponding channel reliability is above 55%.

FIGURE 4 Topographic distribution of the relative channel reliability of (a) the gel-based, and (b) the dry electrode cap, calculated based on the bad channel evaluations for all volunteers and all EEG test sequences
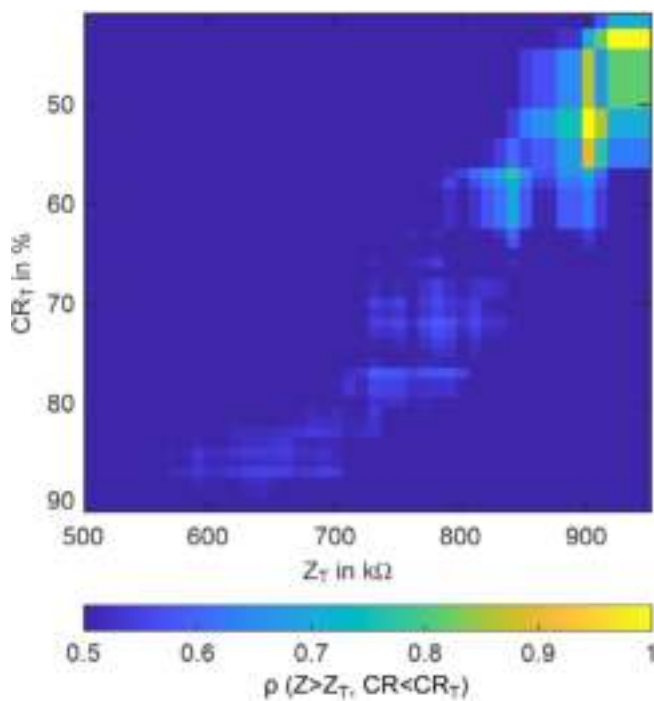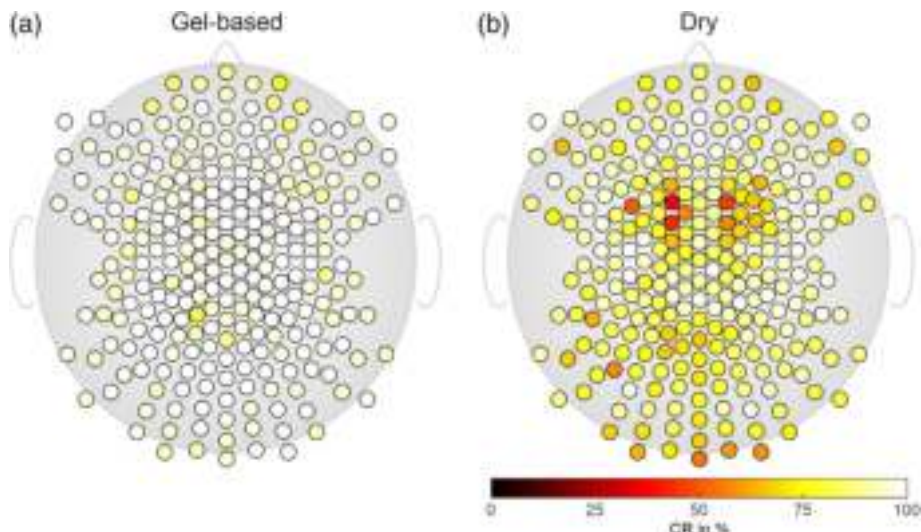
FIGURE 5 Color-coded correlation of channel reliability CR and electrode-skin impedance Z for the dry electrode cap between groups of channels above impedance threshold Z_T and below channel reliability threshold CR_T

3.2 | EEG signal characteristics

The Welch estimation of the resting state EEG PSDs is shown in Figure 6 for the recordings with eyes open (Figure 6a) and eyes closed (Figure 6b) (mean and the standard deviation, calculated across all channels and all volunteers). Moreover, Figure 6c shows the absolute values of the difference between the corresponding recordings with gel-based and dry electrodes. Increased power in the alpha band is visible for both recordings with closed eyes. The alpha band peak

power of the grand average PSD is 10.2 μV^2/Hz and 9.1 μV^2/Hz at 10.1 Hz for the dry and the gel-based recordings, respectively. Increased power for frequencies below 2 Hz is visible for both electrode types in recordings with open eyes compared to recordings with closed eyes. The maximum absolute difference is 3 μV^2/Hz at 1.1 Hz for the resting state EEG recording with closed eyes. For frequencies above 2.1 Hz, the difference of the grand average PSD remains below 1.4 μV^2/Hz. The tests of the individual volunteers' PSDs showed significant differences for the eyes-closed resting state EEG at 3 Hz ($p = .0010$). The p-values for 2 Hz ($p = .0020$) and 4 Hz ($p = .0015$) are low but not below the significance threshold. No significant differences were identified for other frequencies as well. Furthermore, no significant differences were identified for the resting state EEG with open eyes across the complete investigated frequency range.

Figure 7 shows the grand average results of the VEP for all volunteers including a butterfly plot for the individual channels (Figure 7a,b) as well as an overlay plot of the GFPt for the recordings with both electrode types (Figure 7c). The GFPt values of the N75 peaks are 19.3 μV^2/Hz @ 83.0 ms and 20.0 μV^2/Hz @ 78.8 ms for the dry and the gel-based electrodes, respectively. GFPt values for the P100 peaks are 42.0 μV^2/Hz @ 127.4 ms and 43.4 μV^2/Hz @ 124.0 ms for the dry and the gel-based recordings, respectively. The grand averages of the RMSD and correlation coefficient across all channels and volunteers are 0.73 ± 0.16 μV and 0.65 ± 0.08. Channels with high signal amplitudes in the central and parietal area exhibit a high correlation, whereas channels in the low signal amplitude areas exhibit low correlation values. The grand averages for the global field power $RMSD_{GFPt}$ and ρ_{GFPt} are 5.0 ± 1.7 μV and 0.85 ± 0.13. The differences between the corresponding peaks in the GFPt of both electrode types are neither statistically significant for peak power ($p \geq 0.35$) nor peak latency ($p \geq 0.16$).

The grand average SNR_{GFPt} values of the N75 and P100 peaks are 6.0 ± 2.3 and 12.8 ± 4.7 for the gel-based cap versus 5.7 ± 2.1 and 12.7 ± 5.4 for the dry electrode cap, respectively. The grand average SNR_{max} values of the N75 and P100 peaks are 14.8 ± 17.1 and 56.7 ± 58.6 for the gel-based cap versus 12.3 ± 6.9 and 31.6 ± 23.0
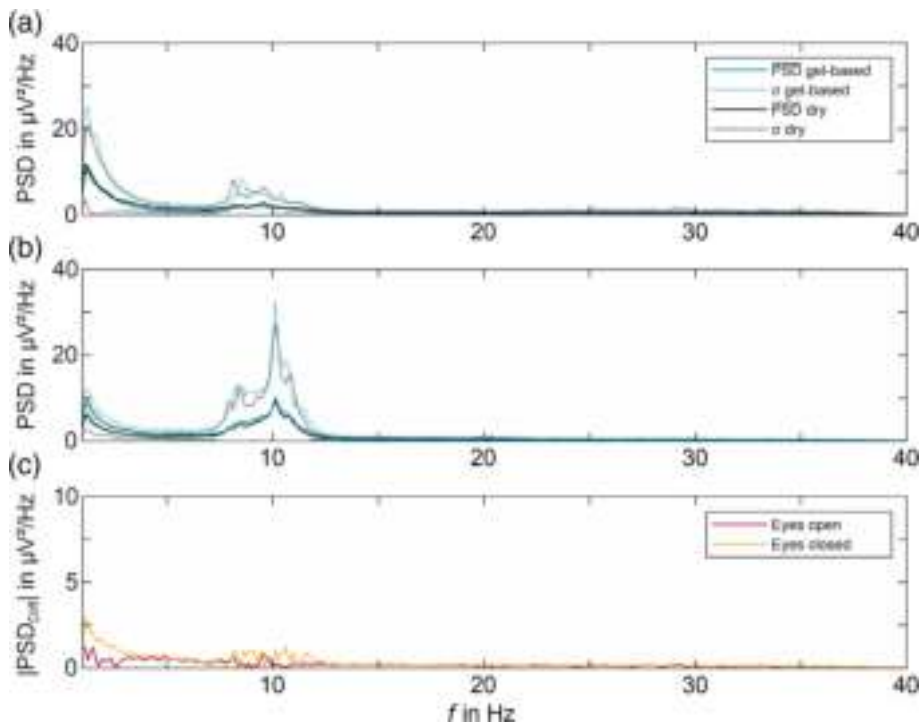
FIGURE 6 Grand average power spectral density (PSD) for the resting state activity recorded with (a) open eyes, and (b) closed eyes for both electrode types. Mean is indicated by solid lines and *SD* is indicated by dotted lines; (c) the absolute value of the difference between gel-based and dry electrode recordings with open or closed eyes
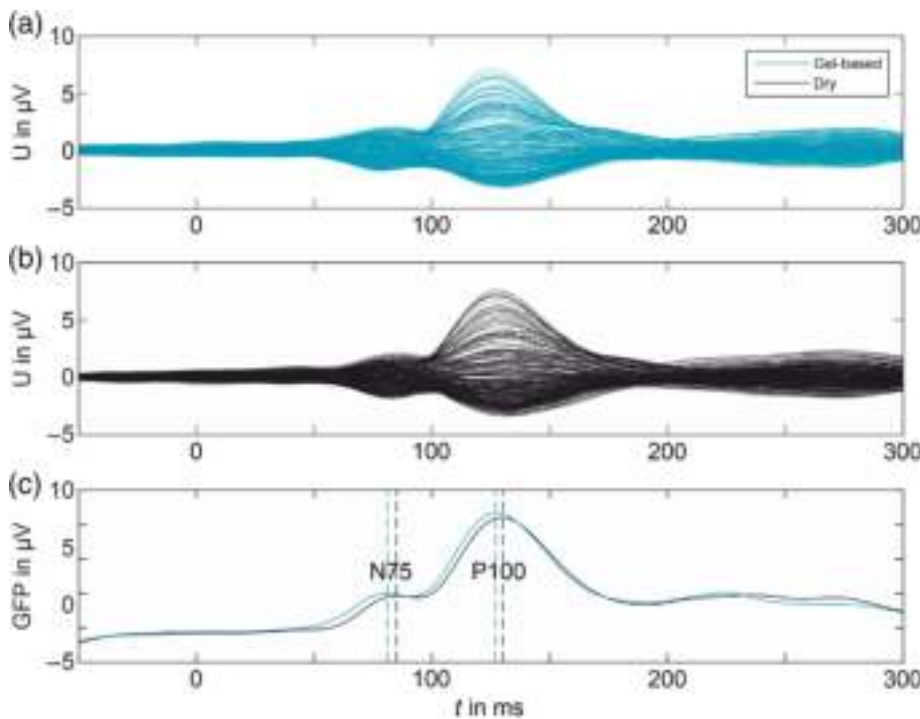

FIGURE 7 Grand average visual evoked potentials (VEP) results: butterfly plots showing all channels of (a) the gel-based recordings, (b) the dry electrode recordings, and (c) an overlay plot of the GFPt traces with highlighted N75 and P100 peak latencies

for the dry cap, respectively. The statistical test showed no significant differences between the SNR_{GFPt} of the gel-based and dry cap for the N75 ($p = .3871$) and the P100 ($p = .4733$) peaks. Furthermore, no significant differences were found between the SNR_{max} of the gel-based and dry cap for the N75 ($p = .9534$) and the P100 ($p = .1526$) peaks. Figure 8 displays violin plots of the distributions of both calculated SNR estimates for the two compared electrode types.

For comparison of the measurements with both electrode types in the spatial domain, we calculated the 2D topographies of the mean alpha band power (Figure 9a) and their absolute difference (Figure 9b). The highest power is visible in the parietal and occipital channels. The difference plot shows an increased difference in the lower occipital area, especially above the left hemisphere. The interpolated maps exhibit statistically significant differences for 2.9% of

FIGURE 8   Violin plots of the SNR distributions of a) SNR_{GFPt}, and b) SNR_{max}, calculated for the visual evoked potentials (VEP) of all subjects. The dots represent individual values. Values outside 2.7 sigma of the data are considered outliers and have been excluded from the violin plots
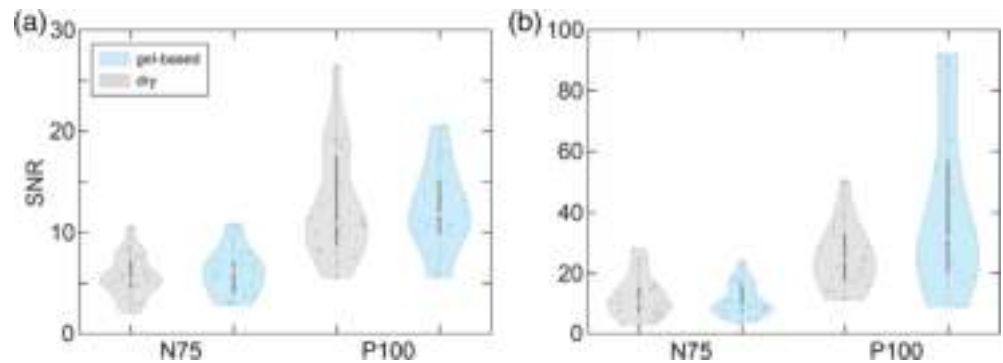
FIGURE 9   Grand average 2D topographic plots of the mean alpha band power in the eyes-closed condition: (a) interpolated plots for the gel-based and dry electrode recordings and (b) absolute difference with areas and channels of statistically significant differences highlighted in red color. White dots in (b) indicate electrode positions without significant differences between recordings with both electrode types
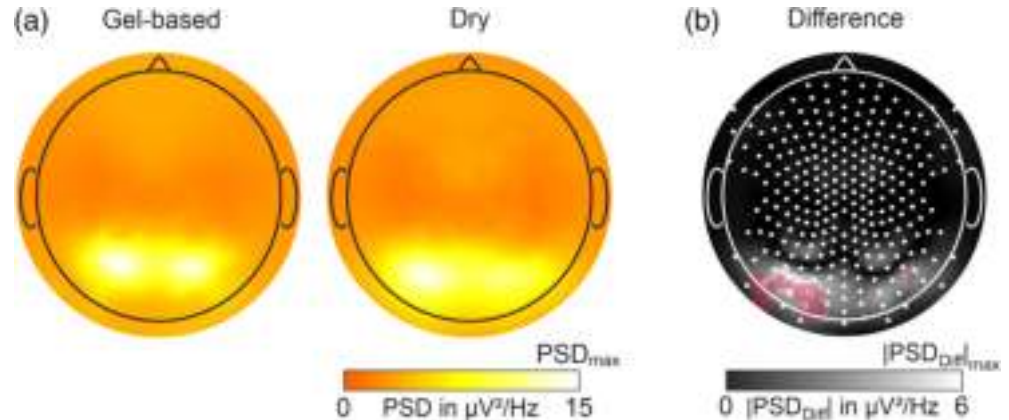
the overall area, whereas the test on the channel level shows only 1.6% of the channels (i.e., four channels) to differ significantly.

A comparison of the VEP peak topographies was performed for their respective peak latencies as shown in Figure 10a for the N75 peak and Figure 10c for the P100 peak. The absolute differences of both topographies are shown in Figures 10b and 9d, respectively. In the case of the N75 peak, 2.8% of the topography and 4.3% of the channels (i.e., 11 channels) differed significantly. For the P100 peak, only 2.1% of the area and 2.3% of the channels (i.e., six channels) differed significantly.

The average preparation time of the gel-based cap was 62 ± 9 min, compared to 19 ± 4 min for the dry electrode cap. The total recording time following the preparation was 29 ± 7 min and 28 ± 7 min, respectively. The attention level (Standford sleepiness scale) reported by the volunteers was 2.3 ± 1.0 for the gel-based cap and 2.6 ± 0.9 for the dry electrode cap prior to the EEG recordings. At the end of the EEG recordings, the volunteers reported attention levels of 3.3 ± 1.2 and 3.5 ± 1.8, respectively. In both cases, the differences between the gel-based and dry caps are nonsignificant ($p = .2863$ prior EEG; $p = .8826$ post EEG).

Asked about the subjective wearing comfort prior to the EEG recordings, the volunteer's rating was 2.5 ± 1.0 and 3.6 ± 1.5 on the 10-point pain scale for the gel-based and the dry cap, respectively. After the EEG recordings, the reported values were 3.0 ± 1.1 and 4.0 ± 1.8. Moreover, the volunteers were asked which one of the two compared cap types they prefer to wear regardless of the prior comfort evaluation. Here, 24 out of the 30 volunteers preferred the dry

electrode cap, compared to 6 volunteers who preferred the gel-based cap.

3.3 | Wearing

Prior to the wearing tests, electrical resistance measurements proved that all test electrodes had an electrical resistivity below 1 Ω for all pins when measured against the back of the baseplate of the electrode.

The resistance measurements for Conditions 1 and 2 (see Table 1) showed no changes and thus no critical wear after 800 and 1,600 applications. After 2,800 applications (Condition 3), four pins at the outer ring of the long pin electrode exhibited loss of coating, whereas all other pins remained with resistances below 1 Ω. Condition 4 yielded the following results after 3,200 applications: 1 electrode showed one pin with loss of coating on the outer ring of pins; one electrode showed two pins with loss of coating on the outer ring of pins; two electrodes showed no loss of coating with all pins exhibiting resistance values below 1 Ω.

For Condition 5, one of the half spheres at the outer rim on the wave pin electrode showed visible loss of the coating at a spot of approximately 0.5 mm in diameter after 3,200 applications. Otherwise, none of the wave pins shows visible damage of the coating. All electrical resistances were still below 1 Ω after the wearing tests.

The SEM images prepared for three electrodes (Conditions 0, 1, and 6) are shown in Figure 11a–c, respectively. The differences visible
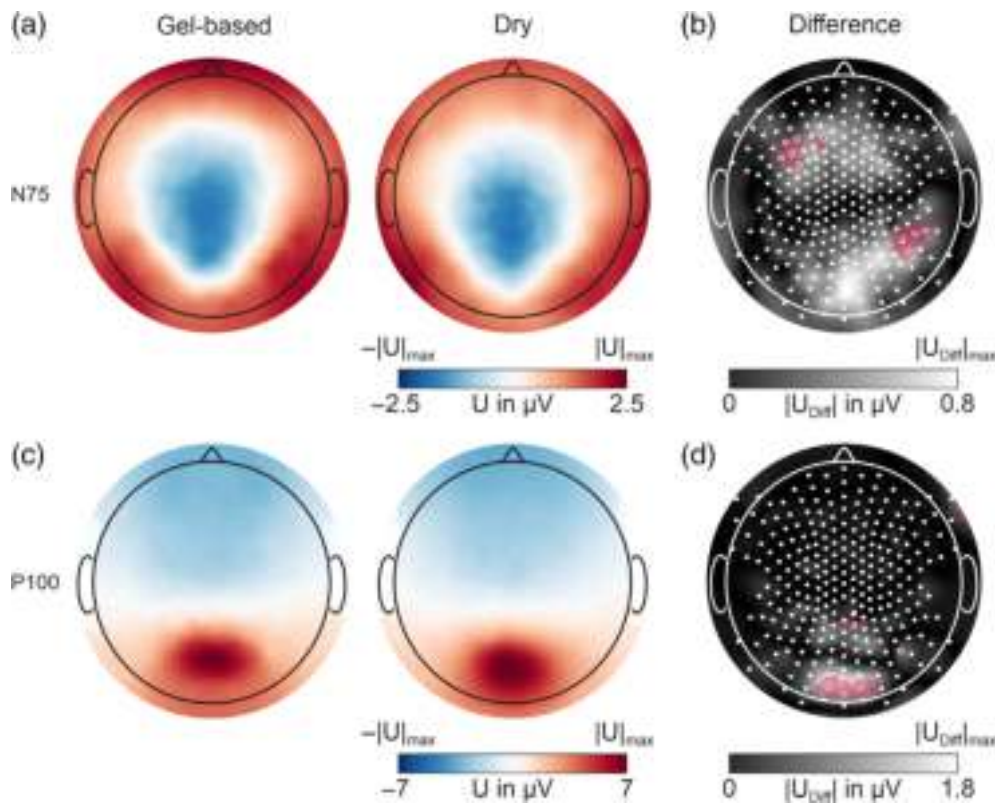
FIGURE 10 Grand average 2D topographic plots of the visual evoked potentials (VEP) main peaks: interpolated plots for the gel-based and dry electrode recordings of (a) the N75, and (c) the P100 peak; (b) absolute difference of the two N75 and (d) P100 topographies. Areas and channels of statistically significant differences are highlighted in red color in (b) and (d), whereas white dots indicate channels without significant differences
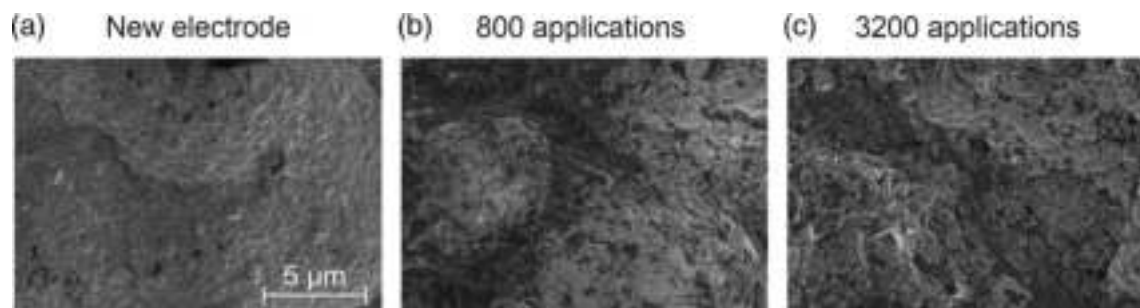
FIGURE 11 SEM surface images for selected conditions of the wearing tests: (a) an unused electrode (Condition 0), (b) after 800 applications on hairy real skin (Condition 1), and (c) after 3,200 applications on artificial skin (Condition 6)

when comparing the three SEM photographs are within the normal variance of the electrodes from different coating batches. Consequently, the two different wearing tests do not show degradation of the surface coating at 800 applications and no surface changes at conductive pins after 3,200 applications.

4 | DISCUSSION

We developed a novel dry electrode cap with 256 electrodes for HD-EEG and successfully validated the cap within an in-vivo study on 30 healthy volunteers. We compared the performance of the new cap to a commercially available gel-based cap using a referential, cascaded amplifier setup. Our results are in line with previous publications

about low-density dry multichannel EEG and prove the functionality and applicability of the novel technology for rapid HD-EEG.

The preparation time of 19 min for the dry electrode cap compared to 62 min for the gel-based cap corresponds to a reduction of 69%. Even though this reduction is lower than in our previous low-density dry EEG study (Fiedler et al., 2015), the reduction is considerable and underlines the applicability of the dry electrode cap for rapid HD-EEG. The difference between both studies may be a result of operator experience. The current study was executed with 4 operators recording 30 datasets, whereas previous studies did not include multiple operators and thus may have profited stronger from increasing proficiency in cap application. Moreover, a reduction of the preparation time of the gel-based caps, that is, an increased preparation speed, increases the risk of overgeling and thus bridging neighboring

electrodes—a completely inexistent risk for a dry electrode cap. Likewise, the post-measurement cleaning efforts are considerably reduced for the dry electrode caps. Volunteers do not need to wash gel out of their hair nor do the operators need to clean individual electrodes from gel remainders. Moreover, in contrast to concepts of semi-dry electrodes (Li, Wu, Yia, He, & Jin, 2020; Mota et al., 2013; Pedrosa et al., 2018), no preparation of individual electrodes is required prior to the cap application. Semi-dry electrodes may show advantages for low-density EEG, but individual electrode preparation renders them similar time-consuming like gel-based electrodes when used for HD-EEG. Of note, the used commercial gel-based reference cap was applied in accordance with the manufacturer recommendations and is designed for fast gel-based cap preparation, not requiring individual skin preparation (i.e., hair separation, skin cleaning, and skin abrasion), but only the application of the electrolyte gel at each electrode. This gel-based cap is, therefore, faster to apply compared to conventional clinical caps requiring the aforementioned additional skin preparation steps. Consequently, the improvement in preparation time using dry electrodes as reported in this study may even be higher when compared to conventional clinical gel-based systems not specifically designed for fast application.

No statistically significant difference between the respective attention levels reported for both cap types is evident. The reported comfort values for the dry electrodes are in line with our previous studies (di Fronso et al., 2019; Fiedler et al., 2015). The adjusted pin height and the wave electrodes at frontal and forehead positions contributed to improved comfort for these head regions as reported by multiple volunteers. The mean comfort ratings are in the lower half of the range 1–10 (i.e., not painful) both for gel-based and dry electrodes, allowing the conclusion that the comfort was sufficient for the recording paradigm at hand. Although the comfort ratings of the dry cap were lower than for the gel-based cap, the overall preference of the majority of volunteers for the dry electrode cap is striking. This fact may be related to (a) the discomfort and time requirements of the gelling and cleaning processes associated with the use of gel-based caps, and (b) the overall wearing time during the paradigm at hand, mimicking the typical dry electrode use case especially for short and intermittent measurements. The polymeric electrode substrate enables future adaptation of the electrode flexibility and implementation of softer electrodes especially at less hairy head positions, contributing to further increased wearing comfort (Fiedler et al., 2018; Kimura et al., 2020).

When selecting the test sequence of gel-based and dry electrode cap, it was necessary to choose between either using a randomized sequence or a fixed sequence always starting with the dry electrode cap. While a randomized sequence generally avoids systematic influences of the test sequence on the results, it would introduce a considerable cross-influence. If the gel-based cap is applied prior to the dry electrodes, the gel changes the skin interface over time due to effects related to skin hydration and chloride deposits, consequently changing the skin properties such as conductivity. Among the various factors influencing the contact properties of dry electrodes skin hydration seems to be an influential one (own unpublished observations). To

avoid such cross-influences, we selected a fixed sequence, always testing the dry electrode cap first. We evaluated the risk and impact of induced errors due to the test sequence being considerably lower than the gel influences on the skin interface and thus the test results.

The electrode-skin impedances before and after the EEG recordings are considerably increased compared to Fiedler et al., 2015. This finding can be assigned to three main reasons:

1. Fiedler et al., 2015 used a different amplifier type. Consequently, the differing impedance measurement frequencies used in both studies resulted in differing impedance values. This difference is likely the main cause of higher impedances, as underlined also by the results of di Fronso et al., 2019 using the same amplifier as the study at hand.
2. The reduced pin number per electrode will contribute to decreasing contact surface and increasing impedance per electrode (Fiedler et al., 2018).
3. The large number of electrodes in an HD-EEG cap results in lower adduction pressure per electrode when using the same fabric and cut, consequently increasing the impedance (Fiedler et al., 2018). This effect is also underlined by the increased impedances in the central and occipital areas of the cap, commonly subject to reduced adduction forces compared to the circumferential electrode positions. A revised cap design will be developed to improve the pressure distribution in the future.

The historic assumption of a direct relationship between electrode-skin impedance and noise level for gel-based recordings has been investigated and rejected for state-of-the-art amplifiers and standard EEG bands below 100 Hz (Scheer, Sander, & Thrams, 2006). However, an often expressed concern when using dry electrodes remains the high impedance level compared to gel-based electrodes. Our results are in line with previous publications and show that high interfacial impedances do not necessarily correlate with bad channels exhibiting high noise levels when using state-of-the-art EEG amplifiers with technical specifications equal to or better than the amplifier model used in this study. For impedances below 800 kΩ, no correlation value above 0.65 was found with respect to channel reliability. Consequently, the higher electrode-skin impedance level did not negatively influence the channel reliability observed. The average channel reliability of 84% is in line with previous publications (di Fronso et al., 2019; Fiedler et al., 2015). A correlation of impedances versus channel reliability results in an impedance of approx. 900 kΩ which may be used as a threshold for practical applications. In multiple cases, individual electrodes with higher impedances still provided good signal quality, indicating that an individual evaluation of signal quality is preferable for dry electrode recordings. The level of the offset potentials for the dry electrodes is below 10 mV (mean) and exhibits a SD below 60 mV. These offsets do not pose limitations when using state-of-the-art amplifier electronics which usually have dynamic ranges per channel above 100 mV.

Our paradigm for comparison of signal characteristics between gel-based and dry electrodes is applicable to laboratory conditions

without movements and provides evidence for equivalence of both electrode types (Fiedler et al., 2015; Marini et al., 2019). Differences in signal characteristics are below 5% in all comparison metrics applied to the EEG recordings of the 84% good channels, supporting the use of the HD-EEG cap for standard clinical and research AC-EEG. Concerning specific EEG applications, automatic artifact and bad channel detection and correction methods may be applied to compensate channel dropouts (Graichen et al., 2015; Mullen et al., 2015; Stone, Tamburro, Fiedler, Haueisen, & Comani, 2018; Tamburro et al., 2018) if required. Channels with low reliability only partially overlap with areas of statistically significant topographic differences. Furthermore, significant differences in the topographies of alpha band power and N75 peak are below 3% and thus lower than in our previous low-density EEG study (Fiedler et al., 2015). Consequently, we conclude that (a) the high spatial resolution of the HD-EEG system does compensate the majority of bad channel dropouts, and (b) further comprehensive bad channel correction is likely required only in case of clustered channel dropouts or in case of investigation of EEG phenomena requiring homogeneous high spatial sampling. The impact of bad channel clustering will be investigated in future studies.

The significant difference observed in the low frequency range of the PSD of resting state EEG with closed eyes is in line with previous observations (Fiedler et al., 2015) and will require further investigation. However, the difference is not observed for the resting state EEG with open eyes and might therefore be a result of the intra-individual variability.

The order of magnitude of the differences in VEP latency and amplitude both fall within intra-individual variability for the used setup (Fiedler et al., 2014; Fiedler et al., 2015). Similar intra-individual latency variability was also reported by Sarnthein, Andersson, Zimmermann, and Zumsteg (2009) for the checkerboard pattern reversal VEP, although for an increased interval between test repetitions. Statistical analysis of the two parameters did not show significant differences between the cap types. Consequently, we do not expect related effects on the practical usability comparing the dry electrode cap versus the gel-based cap.

The extent of the significant differences in the topographies of both the alpha band power as well as the VEPs N75 and P100 peaks is low compared to the overall area and channel number. Differences appear primarily in the occipital, temporal, and lower back areas. These areas are close to the rim of the cap fabric. Differences may be related to (a) positioning errors as a consequence of different cap stretching and adduction characteristics, and (b) lower SNR in the related channels' head region. The different electrode fixation of the dry and gel-based electrodes causes differences in the flexibility of both caps, most prominently impacting electrode positions near the cap's rim. Moreover, isolated areas of topographic differences, not associated with channels exhibiting differences, may be caused by the used interpolation method.

The performed mechanical wearing tests on real and artificial skin underline the reusability and durability of the electrodes. The shown durability of the electrode's coating exceeds the common number of 500 applications during an EEG cap lifecycle as indicated by the manufacturer of the commercial gel-based cap used. The novel electrodes enable reusable HD-EEG caps and thus considerably reduce the costs per application, especially compared to many single-use and/or intrinsically conductive electrode concepts (Bradford et al., 2018; Chen et al., 2014; Fu et al., 2020; Zhang et al., 2020).

Limitations of the current cap and electrode systems will be further investigated and addressed in future studies. The reduced mechanical flexibility of the dry electrode cap, as well as the adduction requirements of the electrodes (Fiedler et al., 2018; Kawana, Yoshida, Kudo, Iwatani, & Miki, 2020; Kimura et al., 2020), require finer grading of the cap sizes for fabric caps or the development of alternative, dedicated cap systems addressing both aspects. Persons with very thick hair (i.e., high hair density and/or hair follicle diameter) may require adapted electrode designs in terms of electrode pin length, density, or orientation. Kawana et al., 2020 studied hair occupancy and orientation, reporting considerable inter- and intraindividual differences suggesting further electrode design optimization. Moreover, the current study was performed under laboratory conditions with the volunteers sitting. Future studies on the impact of movement artifacts need to be executed (di Fronso et al., 2019; Oliveira, Schlink, Hairston, König, & Ferris, 2016). Although the results in the study at hand do not show topological differences of PSDs (alpha activity) and potential distributions (VEPs) in the central head region regardless of higher electrode-skin interfacial impedances, future studies should add a paradigm for detailed analysis of activities related to the central head region, for example, somatosensory and motor activity. As discussed above, high electrode-skin interfacial impedance does not directly correlate with reduced signal quality but may indicate less stable electrode-skin contact. In turn, this may result in a higher susceptibility to movement artifacts which are especially important to consider for mobile EEG applications. An important aspect will be the stabilization and compensation of cable movements and resulting drag forces affecting the cap, specifically considering the high number and thus overall weight of the cables in an HD-EEG cap. Different body positions, for example, during sleep EEG (Leach, Chung, Tüshaus, Huber, & Karlen, 2020) may require adjustment both of the cap layout, and the electrode.

5 | CONCLUSIONS

Dry electrodes allow more degrees of freedom in the design and fabrication of EEG caps and can be self-applied without lengthy preparation or cleaning requirements. The novel dry HD-EEG cap contributes to rapid, gel-free EEG; considerably reduces ecological and economic impact for consumables per HD-EEG measurement, and is the first dry HD-EEG system with 256 channels. Our multi-parameter study provides evidence for the equivalence of the dry and gel-based EEG caps under multiple aspects of signal characteristics in the time, frequency, and spatial domain. The advantages of dry EEG may contribute to new fields of application and increased use of HD-EEG both in research and clinical fields.

CONFLICT OF INTERESTS

Frank Zanow declares that at the time of publication, he is the CEO of eemagine Medical Imaging Solutions GmbH, and stakeholder of the Neuromotion group. eemagine Medical Imaging Solutions GmbH and ANT Neuro B.V. both are subsidiaries of the Neuromotion group.

DATA AVAILABILITY STATEMENT

All raw data used in this publication are available upon request to the corresponding author.

ORCID

Patrique Fiedler https://orcid.org/0000-0001-9196-0717
Carlos Fonseca https://orcid.org/0000-0002-2759-0384
Eko Supriyanto https://orcid.org/0000-0002-6766-793X
Jens Haueisen https://orcid.org/0000-0003-3871-2890

REFERENCES

Astolfi, L., Toppi, J., Fallani, F. D., Vecchiato, G., Salinari, S., Mattia, D., … Babiloni, F. (2010). Neuroelectrical hyperscanning measures simultaneous brain activity in humans. *Brain Topography*, *23*, 243–256. https://doi.org/10.1007/s10548-010-0147-9

Bleichner, M. G., & Debener, S. (2017). Concealed, unobtrusive ear-centered EEG acquisition: cEEGrids for transparent EEG. *Frontiers in Human Neuroscience*, *11*, 163. https://doi.org/10.3389/fnhum.2017.00163

Bradford, J. C., Burke, B., Nguyen, C., Slipher, G. A., Mrozek, R. & Hairston, D. (2018). Performance of conformable, dry EEG sensors. Proceedings of the Annu Int Conf IEEE Eng Med Biol Soc. Honolulu, USA, 2018, pp. 4957–4960. https://doi.org/10.1109/EMBC.2018.8513428

Chen, Y.-H., Op de Beeck, M., Vanderheyden, L., Carrette, E., Mihajlovic, V., Vanstreels, K., … Van Hoof, C. (2014). Soft, comfortable polymer dry electrodes for high quality ECG and EEG recording. *Sensors (Basel)*, *14*(12), 23758–23780. https://doi.org/10.3390/s141223758

Cuadrado, M. L., Valle, B., Fernández-de-las-Peñas, C., Madeleine, P., Barriga, F. J., Arias, J. A., … Pareja, J. A. (2009). Pressure pain sensitivity of the scalp in patients with nummucular headache: A cartographic study. *Cephalalgia*, *30*(2), 200–206. https://doi.org/10.1111/j.1468-2982.2009.01895.x

Dąbrowska, A., Rotaru, G. M., Spano, F., Affolter, C., Fortunato, G., Lehmann, S., … Rossi, R. M. (2017). A water-responsive, gelatine-based human skin model. *Tribology International*, *113*, 316–322. https://doi.org/10.1016/j.triboint.2017.01.027

di Flumeri, G., Aricò, P., Borghini, G., Sciaraffa, N., di Florio, A., & Babiloni, F. (2019). The dry revolution: Evaluation of three different EEG dry electrode types in terms of signal spectral features, mental states classification and usability. *Sensors*, *19*(6), 1365. https://doi.org/10.3390/s19061365

di Fronso, S., Fiedler, P., Tamburro, G., Haueisen, J., Bertollo, M., & Comani, S. (2019). Dry EEG in sports sciences: A fast and reliable tool to assess individual alpha peak frequency changes induced by physical effort. *Frontiers in Neuroscience*, *13*, 982. https://doi.org/10.3389/fnins.2019.00982

Fiedler, P. (2017). *Dry-contact biopotential electrodes: Novel sensor technologies for electroencephalography*. (Dissertation). Technische Universität Ilmenau, Ilmenau/Germany.

Fiedler, P., Haueisen, J., Jannek, D., Griebel, S., Zentner, L., Vaz, F., & Fonseca, C. (2014). Comparison of three types of dry electrodes for electroencephalography. *Acta IMEKO*, *3*(3), 33–37. https://doi.org/10.21014/acta_imeko.v3i3.94

Fiedler, P., Mühle, R., Griebel, S., Pedrosa, P., Fonseca, C., Vaz, F., … Haueisen, J. (2018). Contact pressure and flexibility of multipin dry EEG electrodes. *IEEE Transactions on Neural Systems and Rehabilitation Engineering*, *26*(4), 750–757. https://doi.org/10.1109/TNSRE.2018.2811752

Fiedler, P., Pedrosa, P., Griebel, S., Fonseca, C., Vaz, F., Supriyanto, E., & Haueisen, J. (2015). Novel multipin electrode cap system for dry electroencephalography. *Brain Topography*, *28*, 647–656. https://doi.org/10.1007/s10548-015-0435-5

Filho, E., Bertollo, M., Robazza, C., & Comani, S. (2015). The juggling paradigm: A novel social neuroscience approach to identify neuropsychophysiological markers of team mental models. *Frontiers in Psychology*, *6*, 799. https://doi.org/10.3389/fpsyg.2015.00799

Fonseca, C., Silva Cunha, J. P., Martins, R. E., Ferreira, V. M., Marques de Sa, J. P., Barbosa, M. A., & Martins da Silva, A. (2007). A novel dry active electrode for EEG recordings. *IEEE Transactions on Biomedical Engineering*, *54*(1), 162–165. https://doi.org/10.1109/TBME.2006.884649

Fu, Y., Zhao, J., Dong, Y., & Wang, X. (2020). Dry electrodes for human bioelectrical signal monitoring. *Sensors*, *20*, 3651. https://doi.org/10.3390/s20133651

Graichen, U., Eichardt, R., Fiedler, P., Strohmeier, D., Zanow, F., & Haueisen, J. (2015). SPHARA—A generalized spatial Fourier analysis for multi-sensor systems with non-uniformly arranged sensors: Application to EEG. *PLoS One*, *10*(4), e0121741. https://doi.org/10.1371/journal.pone.0121741

Grozea, C., Voinescu, C. D., & Fazli, S. (2011). Bristle-sensors—Low-cost flexible passive dry EEG electrodes for neurofeedback and BCI applications. *Journal of Neural Engineering*, *8*(2), 25008. https://doi.org/10.1088/1741-2560/8/2/025008

Hinrichs, H., Scholz, M., Baum, A. K., Kam, J. W. Y., Knight, R. T., & Heinze, H.-J. (2020). Comparison between a wireless dry electrode EEG system with a conventional wired wet electrode EEG system for clinical applications. *Scientific Reports*, *10*, 5218. https://doi.org/10.1038/s41598-020-62154-0

Hoddes, E., Dement, W., & Zarcone, V. (1972). The developent and use of the Stanford sleepiness scale (SSS). *Psychophysiology*, *9*, 150.

Kawana, T., Yoshida, Y., Kudo, Y., Iwatani, C., & Miki, N. (2020). Design and characterization of an EEG-hat for reliable EEG measurements. *Micromachines*, *11*, 635. https://doi.org/10.3390/mi11070635

Kimura, M., Nakatani, S., Nishida, S.-I., Taketoshi, D., & Araki, N. (2020). 3D printable dry EEG electrodes with coiled-spring prongs. *Sensors*, *20*, 4733. https://doi.org/10.3390/s20174733

Kleffner-Canucci, K., Lu, P., Naveway, J. D., & Tucker, J. D. (2012). A novel hydrogel electrolyte extender for rapid application of EEG sensors and extended recordings. *Journal of Neuroscience Methods*, *206*, 83–87. https://doi.org/10.1016/j.jneumeth.2011.11.021

Larson, E., & Taulu, S. (2017). Reducing sensor noise in MEG and EEG recordings using oversampled temporal projection. *IEEE Transactions on Biomedical Engineering*, *65*(5), 1002–1013. https://doi.org/10.1109/TBME.2017.2734641

Lascano, A. M., Lalive, P. H., Hardmeier, M., Fuhr, P., & Seeck, M. (2017). Clinical evoked potentials in neurology: A review of technuiques and indications. *Journal of Neurology, Neurosurgery, and Psychiatry*, *88*(8), 688–696. https://doi.org/10.1136/jnnp-2016-314791

Lau-Zhu, A., Lau, M. P. H., & McLoughlin, G. (2019). Mobile EEG in research on neurodevelopmental disorders: Oportunities and challenges. *Developmental Cognitive Neuroscience*, 36, 100635. https://doi.org/10.1016/j.dcn.2019.100635

Leach, S., Chung, K., Tüshaus, L., Huber, R., & Karlen, W. (2020). A protocol for comparing dry and wet EEG electrodes during sleep. *Frontiers in Neuroscience*, 14, 586. https://doi.org/10.3389/fnins.2020.00586

Lepola, P., Myllymaa, S., Töyräs, J., Muraja-Murro, A., Mervaaala, E., Lappalainen, R., & Myllymaa, K. (2014). Screen-printed EEG electrode set for emergency use. *Sensors and Actuators, A: Physical*, 213, 19–26. https://doi.org/10.1016/j.sna.2014.03.029

Li, G. L., Wu, J.-T., Yia, Y.-H., He, Q.-G., & Jin, H.-G. (2020). Review of semi-dry electrodes for EEG recording. *Journal of Neural Engineering*, 17, 51004. https://doi.org/10.1088/1741-2552/abbd50

Liu, Q., Ganzetti, M., Wenderoth, N., & Mantini, D. (2018). Detecting large-scale brain networks using EEG: Impact of electrode density, head modeling and source localization. *Frontiers in Neuroinformatics*, 12, 4. https://doi.org/10.3389/fninf.2018.00004

Makeig, S., Gramann, K., Jung, T.-P., Sejnowski, T. J., & Poizner, H. (2009). Linking brain, mind and behaviour. *International Journal of Psychophysiology*, 73, 95–100. https://doi.org/10.1016/j.ijpsycho.2008.11.00

Marini, F., Lee, C., Wagner, J., Makeig, S., & Gola, M. (2019). A comparative evaluation of signal quality between a research-grade and a wireless dry-electrode mobile EEG system. *Journal of Neural Engineering*, 16, 54001. https://doi.org/10.1088/1741-2552/ab21f2

Mota, A. R., Duarte, L., Rodrigues, D., Martins, A. C., Machado, A. V., Vaz, F., ... Fonseca, C. (2013). Development of a quasi-dry electrode for EEG recording. *Sensors and Actuators, A: Physical*, 199, 310–317. https://doi.org/10.1016/j.sna.2013.06.013

Mullen, T. R., Kothe, C. A. E., Chi, M., Ojeda, A., Kerth, T., Makeig, T., ... Cauwenberghs, G. (2015). Real-time neuroimaging and cognitive monitoring using wearable dry EEG. *IEEE Transactions on Biomedical Engineering*, 62(11), 2553–2567. https://doi.org/10.1109/TBME.2015.2481482

Oliveira, A. S., Schlink, B. R., Hairston, W. D., König, P., & Ferris, D. P. (2016). Induction and separation of motion artifacts in EEG data using a mobile phantom head device. *Journal of Neural Engineering*, 13, 36014. https://doi.org/10.1088/1741-2560/13/3/036014

Patki, S., Grundlehner, B., Verwegen, A., Mitra, S., Xu, J., Matsumoto, A., ... Penders, J. (2012). Wireless EEG system with real time impedance monitoring and active electrodes. Proceedings of the IEEE Biomedical Circuits and Systems Conference. Hsinchu, Taiwan, 2012, pp. 2163–4025. https://doi.org/10.1109/BioCAS.2012.6418408

Pedrosa, P., Fiedler, P., Pestana, V., Vasconcelos, B., Gaspar, H., Amaral, M. H., ... Fonseca, C. (2018). In-service characterization of a polymer wick-based quasi-dry electrode for rapid pasteless electroencephalography. *Biomedical Engineering*, 63(4), 349–359. https://doi.org/10.1515/bmt-2016-0193

Perrin, F., Pernier, J., Bertrand, O., & Echallier, J. F. (1989). Spherical splines for scalp potential and current density mapping. *Electroencephalography and Clinical Neurophysiology Supplement*, 72, 184–187. https://doi.org/10.1016/0013-4694(89)90180-6

Puce, A., & Hämäläinen, M. A. (2017). A review of issues related to data acquisition and analysis in EEG/MEG studies. *Brain Sciences*, 7(6), 58. https://doi.org/10.3390/brainsci7060058

Ramon, C., & Holmes, M. D. (2015). Spatiotemporal phase clusters and phase synchronization patterns derived from high density EEG and ECoG recordings. *Current Opinion in Neurology*, 31, 127–132. https://doi.org/10.1016/j.conb.2014.10.001

Ramon, C., & Holmes, M. D. (2020). Increased phase cone turnover in 80-250 Hz bands occurs in the epileptogenic zone during Interictal periods. *Frontiers in Human Neuroscience*, 14, 615744. https://doi.org/10.3389/fnhum.2020.615744

Robinson, A. K., Venkatesh, P., Boring, M. J., Tarr, M. J., Pulkit, G., & Behrmann, M. (2017). Very high density EEG elucidates spatiotemporal aspects of early visual processing. *Scientific Reports*, 7, 16248. https://doi.org/10.1038/s41598-017-16377-3

Sarnthein, J., Andersson, M., Zimmermann, M. B., & Zumsteg, D. (2009). High test-retest reliability of checkerboard reversal visual evoked potentials (VEP) over 8 months. *Clinical Neurophysiology*, 120, 1835–1840. https://doi.org/10.1016/j.clinph.2009.08.014

Scheer, H. J., Sander, T., & Thrams, L. (2006). The influence of amplifier, interface and biological noise on signal quality in high-resolution EEG recordings. *Physiological Measurement*, 27(2), 109–117. https://doi.org/10.1088/0967-3334/27/2/002

Scott, J., & Huskisson, E. C. (1976). Graphic representation of pain. *Pain*, 2(2), 175–184.

Searle, A., & Kirkup, L. (2000). A direct comparison of wet, dry and insulating bioelectric recording electrodes. *Physiological Measurement*, 21, 271–283. https://doi.org/10.1088/0967-3334/21/2/307

Skrandies, W., & Lehmann, D. (1982, 1982). Occurence time and scalp location of components of evoked EEG potential fields. In W. M. Herrmann (Ed.), *Electroencephalography in drug research*. Stuttgart, Germany: Fischer.

Sohrabpour, A., Lu, Y., Kankirawatana, P., Blount, J., Kim, H., & He, B. (2016). Effect of EEG electrode number on epileptic source localization in pediatric patients. *Clinical Neurophysiology*, 126(3), 472–480. https://doi.org/10.1016/j.clinph.2014.05.038

Stone, D. B., Tamburro, G., Fiedler, P., Haueisen, J., & Comani, S. (2018). Automatic removal of physiological artifacts in EEG: The optimized fingerprint method for sports science applications. *Frontiers in Human Neuroscience*, 12, 96. https://doi.org/10.3389/fnhum.2018.00096

Stoyell, S. M., Wilmskoetter, J., Dobrota, M.-A., Chinappen, D. M., Bonhilha, L., Mintz, M., ... Chu, C. J. (2021). High-density EEG in current clinical practice and opportunities for the future. *Clinical Neurophysiology*, 38(2), 112–123. https://doi.org/10.1097/WNP.0000000000000807

Tamburro, G., Fiedler, P., Stone, D., Haueisen, J., & Comani, S. (2018). A new ICA-based fingerprint method for the automatic removal of physiological artifacts from EEG recordings. *PeerJ*, 6, e4380. https://doi.org/10.7717/peerj.4380

van Rijn, C. M., Peper, A., & Grimbergen, C. A. (1990). High-quality recording of bioelectric events. Part I. interference reduction theory and practice. *Medical & Biological Engineering & Computing*, 28(5), 389–397. https://doi.org/10.1007/BF02441961

Xu, J., Mitra, S., van Hoof, C., Yazicioglu, R. F., & Makinwa, K. A. A. (2017). Active electrodes for wearable EEG acquisition: Review and electronics design methodology. *IEEE Reviews in Biomedical Engineering*, 10, 187–198. https://doi.org/10.1109/RBME.2017.2656388

Zhang, L., Kumar, K. S., He, H., Cai, C. J., He, X., Gao, H., ... Ouyang, J. (2020). Fully organic compliant dry electrodes selfadhesive to skin for long-term motion-robust epidermal biopotential monitoring. *Nature Communications*, 11, 4683. https://doi.org/10.1038/s41467-020-18503-8